RICE UNIVERSITY

A 3.0 meter Liquid Mirror Telescope

by

Mark Mulrooney

A THESIS SUBMITTED
IN PARTIAL FULFILLMENT OF THE
REQUIREMENTS FOR THE DEGREE

Doctor Of Philosophy

APPROVED, THESIS COMMITTEE:

_____
Reginald J. Dufour, Professor, Chair
Physics and Astronomy

_____
Jon C. Weisheit, Adjunct Professor
Physics and Astronomy
Los Alamos National Laboratory

_____
Paul A. Cloutier, Professor
Physics and Astronomy

_____
Richard H. Gomer, Professor
Biochemistry and Cell Biology

HOUSTON, TEXAS
SEPTEMBER, 2000

ABSTRACT

A 3.0 meter Liquid Mirror Telescope

by

Mark Mulrooney

We constructed a 3.0 meter diameter f/1.5 Liquid Mirror Telescope (LMT) between 1990 and 1994 at the NASA Johnson Space Center, Houston, Texas. We have subsequently operated it since 1995 at the NASA Orbital Debris Observatory (NODO), Cloudcroft, NM. Employing an inexpensive rotating container of mercury as its primary parabolic mirror, the NASA-LMT is a cost-effective alternative to telescopes utilizing glass mirrors. We detail criteria for mirror construction including environmental considerations via Hg vapor emission analysis. We describe performance optimization to the NODO site seeing limit of 0.8 arcseconds FWHM via analysis of perturbations to image quality from mirror angular velocity stability, dynamic balance, rotational axis tilt, and prime focus lateral and tilt displacements. We detail the behavior of the two prominent mirror surface wave phenomena - spiral and concentric forms. We demonstrate that the former probably results from vorticity in the air boundary layer above the mirror and show diffraction effects from the latter. We describe mirror stabilization in terms of boundary layer theory.

The prime focus NASA-LMT utilizes corrective optics yielding a field of 46 arcminute diameter. Utilizing Micro-Channel-Plate (MCP) intensified video cameras we

have obtained 750 hours of zenith staring orbital object event data with a limiting object diameter of approximately 1 cm at 1000 km altitude and 0.1 albedo. We have extended to 17.75 the lower magnitude limit of optical detections among the telescopes employed for orbital object surveys, further demonstrated the incompleteness of the SATCAT, and corroborated results of RADAR employed in orbital object detection.

Utilizing CCDs we have conducted a 135 night broadband and multi-narrowband survey of 20 square degrees of sky at high galactic latitude down to a limiting magnitude of ~22.0. The survey data will yield information on object morphology, spectral classifications, and large-scale structure to a redshift (z) of 0.5 with an accuracy of $\Delta z \leq 0.02$. Broadband images from this survey are presented, demonstrating that the NASA-LMT optical performance is comparable to conventional telescopes of equivalent size located at a similar site.

ACKNOWLEDGEMENTS

The success of the NASA-LMT is due to the efforts of a great many individuals. Without Ermanno Borra's pioneering efforts, Drew Potter's willingness to gamble on an incompletely vetted technology, Eugene's Dahl's steadfast conviction that the PICo air bearing would handily fulfill the requisite stability and capacity requirements, Harvey Richardson's brilliant optical designs and Martin High's fabrication team, and Paul Hickson's extraordinary willingness not only to construct the mirror container, but to donate his uniquely enlightened advice and assistance time and again over the past decade, the NASA-LMT would not exist, let alone have achieved the level of refinement and performance exhibited herein. Similarly, without the machining skills of Bill Davidson, the military precision of Freeman Bertrand, and the engineering acumen of Terry Byers and Frank Gibbons, the NASA effort would have faltered shortly after conception. Born of the close collaborations and the ultimate success of the project, the friendships formed with these exceptional individuals have been equally stellar.

The same is true of the many other participants in the project, including my friend and former Lockheed manager Pat Jones who gave me the opportunity of a lifetime despite my youth, the late Karl Henize who conveyed a sense of delight in the pursuit of knowledge that remains within me, Barbara Nowakowski who not only processed orbital object data, but also supplied frequent moral support and encouragement, and Christine O'Neill whose management style and keen interest in the project's success completely reinvigorated the effort on more than one occasion.

Thanks go also to Bob Weggeman for the numerous wiring tasks performed at JSC, to Jerry Hanes for his kindness and support, Glen Cress for his extraordinary efforts to retain project funding as NODO operations advanced to an efficient data acquisition state, to John Africano who through his data analysis prowess and love of astronomy ostensibly, along with Eugene Stansbery, rescued the NASA-LMT from funding oblivion, and to Ralph Wuerker for his enthusiasm and vision in recognizing the potential of the LMT and translating it to his own highly successful LIDAR.

NODO operations would not have been possible without the infrastructure support of the National Solar Observatory (NSO). Rex Hunter generously facilitated NASA's use of the NODO Cloudcroft Facility when he could have just as easily declined our inquiries. Barring the use of this site, the available alternatives would have led to almost certain failure. The NSO Civil Engineering team of Robert Rentschler, Will and Mike Rogers, Roy Shimming and Bruce Smaga performed a first class renovation of the NODO facility prior to NASA's occupation. Robert especially, with whom I share kindred sensibilities, has rescued numerous nights of observing which would otherwise have been lost to a jammed dome slit, power failures, or myriad other facility malfunctions. Gratitude goes to Gary Montana for rapidly mastering NODO WinTel PC and networking tasks and salvaging countless crashed PCs and their sometimes invaluable data. Thanks also go to Scott Gregory for his skill as a machinist and his insight into aesthetic mechanical design. A heartfelt thank you also goes to our chief observer Anna Scott who for the past three years has almost single-handedly acquired the orbital object data and a large portion of the astronomical data, including much of that

presented in Chapter VI.

On a personal note I would like to thank my thesis advisor and friend Reginald Dufour for believing in me and supporting my efforts despite the persistent delays and procrastinations. I can only hope the end product mitigates the patience expended. I would similarly like to thank Jon Weisheit for his friendship and helping to imbue in me a sense of accomplishment and well-being despite my lengthy route to thesis completion. My warmest thanks also go to Maria Byrne and Umbe Cantu whose support of my endeavors has been unfaltering since my undergraduate days 15 years ago. And I owe inestimable gratitude to Patricia Reiff who seven months ago spurred me to completion when I might otherwise have continued piecemeal, focusing on other tasks, and likely missed the objective. And a warm thank you to Ray Smartt who during thesis completion gave me frequent reassurance and guidance.

Of course none of my efforts with respect to the NASA-LMT or the thesis would have reached fruition without the unwavering love and support of my parents, Maureen and Joe, and of my sisters, Elizabeth and Sharon. A special note of thanks also goes to my friend and confidant Marilyn Garber who helps lend peace to my spirit and reinforces the belief that anything we imagine is possible.

TABLE OF CONTENTS

LIST OF TABLES

LIST OF FIGURES

PREFACE

This thesis discusses the construction, operation, and scientific utility of a 3.0 meter diameter Liquid Mirror Telescope (LMT) built by the National Aeronautics and Space Administration (NASA) for the gathering of orbital object and astronomical data. The NASA-LMT is a low-cost optical telescope whose primary mirror consists of a rotating container of liquid mercury (Hg; from the Greek Hydrargyrum). It is the centerpiece of the NASA Orbital Debris Observatory (NODO) located in Cloudcroft, New Mexico (Figures P-1 through 3). At the time of this writing (2000), the NASA-LMT holds the distinction of having the longest operating record for an astronomical LMT - it recently completed its sixth consecutive year of data acquisition.

Because of the unique nature of this type of instrument and the circumstances of its relatively recent development, it was decided that the description herein should be as comprehensive as possible in an effort to consolidate for researchers the fundamental aspects of LMT construction, operations, and capabilities. Extensive experience with the NASA-LMT from initial conception to fully operational status has made possible a thorough treatment of various engineering aspects of the LMT as well as a demonstration of the optical performance and scientific utility of the instrument. The latter aspect is essential, as it firmly distinguishes the LMT as a powerful research tool as opposed to an interesting novelty. The former is equally relevant, as it describes some of the latest advancements in LMT construction and operation and will be of assistance, along with an increasing body of literature, to those building or contemplating construction of a LMT.

Integration of instrument development and a demonstration of its capabilities into a coherent document was facilitated by the concurrent nature of the work performed. Much of the hardware troubleshooting and instrument refinement were conducted while research data was being acquired. The NASA-LMT addressed herein is evolving continually as is the nature of its data products - the two are intertwined.

The text is divided into six parts:

Chapter I discuses the development of the LMT focussing on the pioneering work of other researchers in the development of both historical and contemporary instruments.

Chapter II describes the development and scientific impetus for the NASA-LMT initially driven by NASA's mandate to study the orbital debris environment and culminating in a fully operational telescope capable of a variety of scientific endeavors.

Chapter III addresses the properties of the rotating fluid in terms of the surface aberrations induced by the spherical rotating earth, the relationship between mirror angular velocity stability and optical resolution, and the wave phenomena observed on the mirror surface.

Chapter IV describes the fundamentals of the instrument's construction and optimization including engineering specifications for the mirror subsystem, optical specifications for

the prime focus assembly, and detector characteristics.

Chapter V describes NASA-LMT operations ranging from alignment procedures to mirror cleaning. Numerous sample images are presented to illustrate various aspects of LMT optical performance.

Chapter VI consists of demonstrations of the LMT's viability for scientific inquest. A gallery of sample images is presented and current astronomical and orbital object survey projects are discussed.

3.0 m NASA-LMT

Figure P-1. View of the NASA-LMT inside the main dome at the NODO location. The wide-angle lens used for this photograph gives a curved appearance to the straight legs supporting the prime focus assembly. Polyethylene tarps used for mercury containment surround the mirror and the mercury vacuum cleaner can be seen to the author's left in the rear of the photo. The conical assembly visible at prime focus is the 4-element corrector lens that removes coma and astigmatism and flattens the field of the f/1.5 parabola. The mirror is spinning in this photo at its nominal rate of approximately 10 revolutions per minute (rpm). Photo courtesy Chip Simons.

NASA Orbital Debris Observatory (NODO), Cloudcroft, NM

Figure P-2. Aerial view of the northeast face of the NASA Orbital Debris Observatory (NODO) located 3 kilometers north of Cloudcroft, New Mexico at an altitude of 2772 m above mean sea level (AMSL). The 4.5m wide hemispherical slit of the 14.5m diameter main dome is clearly visible. The two diagonally opposed 3m diameter secondary domes are visible at the north (left) and south corners of the building. Two individuals are visible at the bottom left, giving a sense of scale. Photo courtesy Anna Scott.

NASA Orbital Debris Observatory (NODO), Cloudcroft, NM

Figure P-3. Day and night views of southeast face of the NASA Orbital Debris Observatory (NODO). The upper image shows the 4.5m wide hemispherical slit of the 14.5m diameter main dome in the fully extended position with the interior windscreen visible. The top of the high-bay door leading to the 1000 m^2 building interior is visible left of bottom center and the entry door is visible to the right. Both images show one of the two secondary domes at the building south corner.

CHAPTER I

INTRODUCTION

It is well known and straightforward to demonstrate that the equilibrium surface configuration of a rotating fluid, whose axis is parallel to a uniform gravitational field, is a paraboloid whose focal length is determined by the angular velocity of rotation (ω) and the gravitational acceleration (g). Referencing Figure I-1, and balancing Normal (N), Centrifugal (F_c), and Gravitational (F_g) forces on a mass element (m), we have:

$$F_g = mg \equiv N_Z = N\cos\theta \qquad \text{(gravitational force balance)} \qquad \text{(I.a)}$$

$$F_C = mr\varpi^2 \equiv N_R = N\sin\theta \qquad \text{(centrifugal force balance)} \qquad \text{(I.b)}$$

We also note:

$$\frac{dz}{dr} = \tan\theta \qquad \Rightarrow \qquad \frac{dz}{dr} = \frac{r\omega^2}{g} \qquad \Rightarrow \qquad z = \frac{\omega^2}{2g}r^2 \qquad \text{(I.c)}$$

The last equation can be written in the form of a parabola:

$$z = \frac{1}{4F}r^2 \qquad \text{(I.d)}$$

Parabolic Equilibrium Surface of a Rotating Fluid

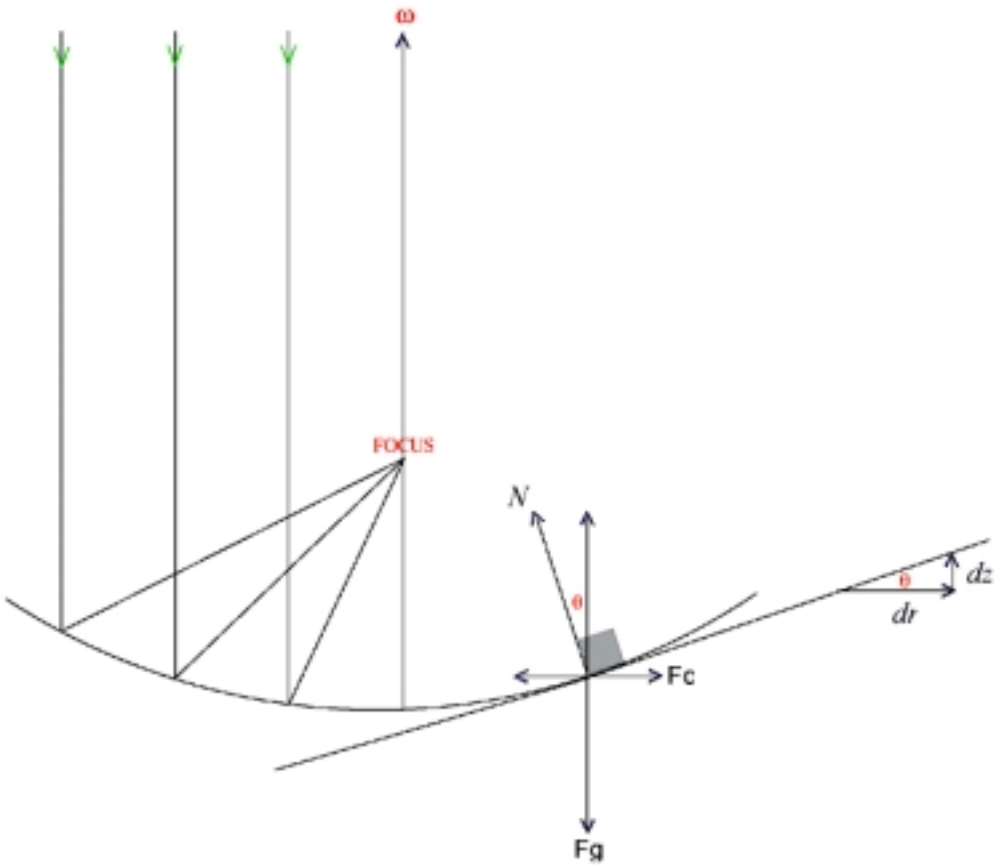

Figure I-1. Schematic drawing illustrating the dominant forces acting upon a rotating fluid element. The fluid rotates about the central vertical axis and is acted upon by centrifugal force and gravity. Force balance yields a parabolic equilibrium surface with focal length: $F = g/2\omega^2$

With focal length:

$$F = \frac{g}{2\omega^2} \qquad \text{(I.e)}$$

This is the zeroth order solution to the equilibrium surface. In Chapter III we will introduce higher order terms.

Since paraboloids have the unique property of focusing to a point axial parallel light rays from infinity (such as those originating from stars), it would appear that a simple means by which a telescope mirror can be created is to take a container full of a reflective fluid such as mercury (Hg), and spin it at constant angular velocity about a central axis parallel to the local gravitational vector (Figures I-2 and 3). This obviates the expensive and painstaking process of grinding and figuring a glass mirror - making possible large, fast-focal ratio, cost-effective astronomical telescopes. These attributes provide the primary motivation for LMT development and enable their potential wide-spread use in astronomy.

The first published reference to a LMT appears to be a letter from Ernesto Capocci of the Naples Observatory that was read before the Royal Academy of Belgium in 1850 (Gibson 1990; Mailly 1872), but because of technical challenges, almost 60 years would pass before a liquid mirror telescope trained on the heavens would be built and another 85 years hence before an astronomical quality LMT would be constructed.

The first well-documented experimental liquid mirror was a 0.35 meter diameter

NASA-LMT: 3.0 m Mirror

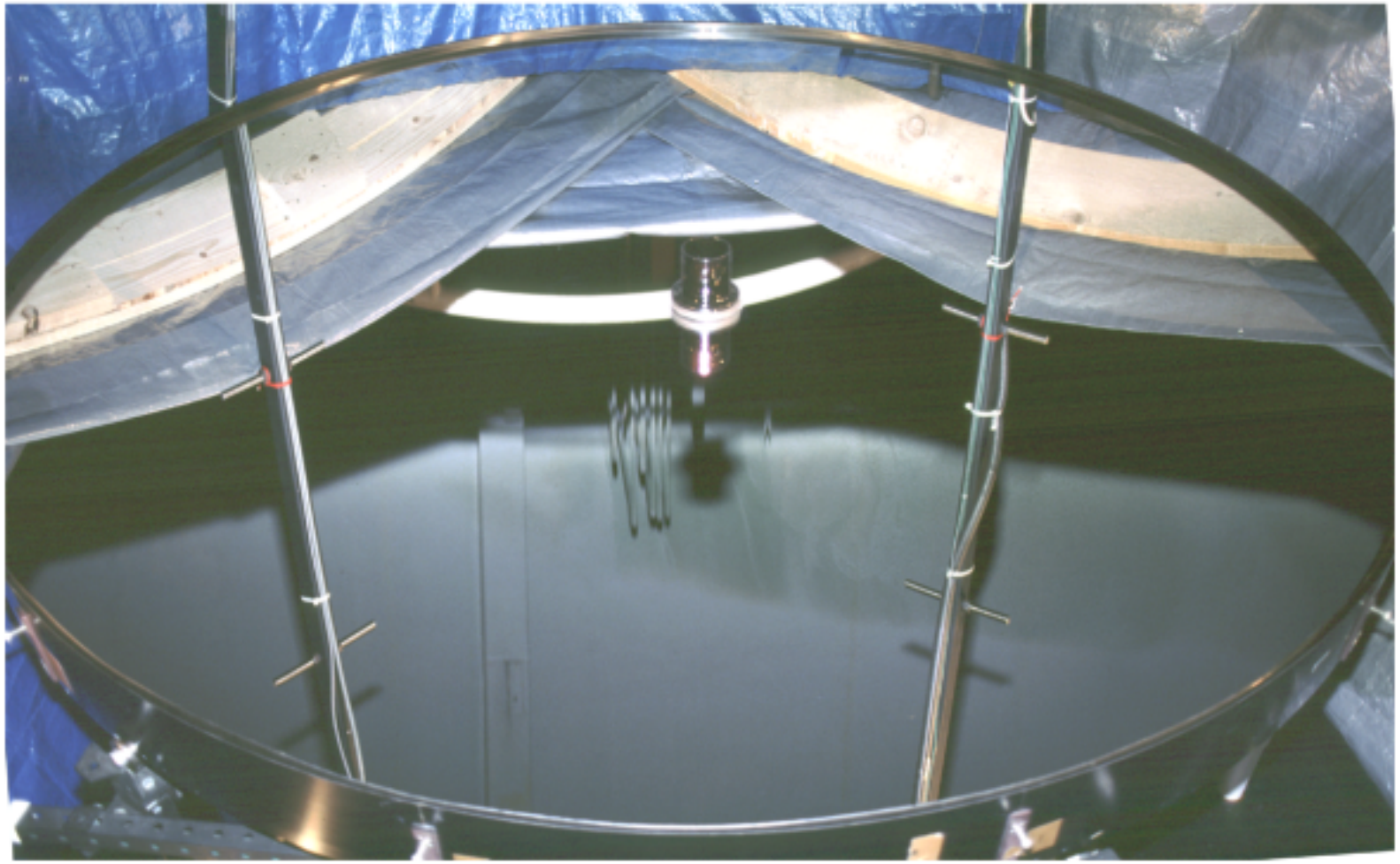

Figure I-2. Close-up of the 3.0 m diameter NASA Liquid Mirror. The mirror is spinning at an angular velocity (ω) of 1.043107 radians/second yielding a parabolic surface with a 4.511 m focal length (f/1.503) at the NODO location (g=9.8167 m/s^2).

NASA-LMT: 3.0 m Mirror

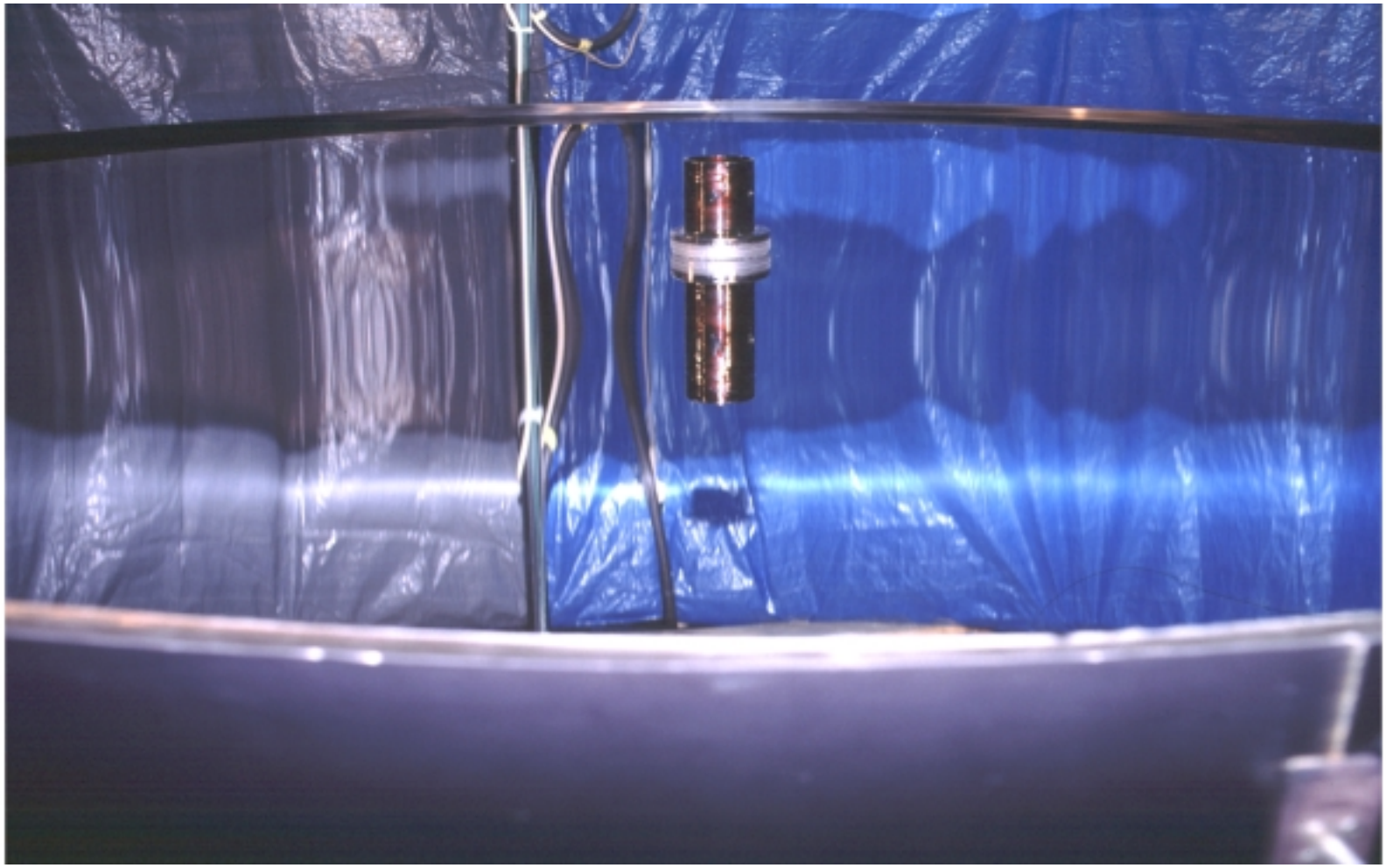

Figure I-3. Close-up of the 3.0 m diameter NASA Liquid Mirror. The deep (f/1.5) concave parabolic figure is evident. The sagitta (center depression relative to mirror perimeter) is 12.5 centimeters.

laboratory instrument constructed in 1872 by Henry Skey (Skey 1874; Gibson 1990). With it Skey was able to image test objects and demonstrate empirically the dependence of focal length on mirror angular velocity. A belt-drive mechanism (which inhibited the transmission of motor vibrations to the mirror) was used to maintain rotation of a Hg filled platter resting on a mechanical bearing platform. The drives included a pendulum-regulated electromagnetic engine and a water-driven hydroelectric turbine, neither of which provided the speed stability necessary for astronomical imaging. Skey's LMT probably appeared as a simplified version of the modern belt-driven 2.7m LMT developed by the University of British Columbia (UBC) shown schematically in Figure I-4 and discussed later in this chapter (Hickson 1994a).

Experiments with LMTs paused until Robert Wood of Johns Hopkins University built a 0.18 meter laboratory liquid mirror in 1908. He used it as a prototype to study liquid mirror properties before building a larger 0.51 meter LMT intended for astronomical observations (Wood 1909; Gibson 1990). The larger instrument utilized a mechanical bearing to support a rotating Hg-filled platter and an unsynchronized 110V AC motor with an India-rubber drive belt to minimize transmitted vibrations from the motor. To isolate it from environmental sources of vibration, the LMT was mounted on a concrete pad at the bottom of a 4 meter deep pit. Even with this precaution Wood commented that he could detect ripples on the mirrors surface correlated with carriage traffic nearby – hinting at the extreme sensitivity of liquid mirrors to vibration. Despite this simple arrangement Wood achieved a remarkable result: he was able to achieve sufficient short-term stability with his LMT that he resolved the double-double star

Schematic of the 2.7 m UBC/Laval Belt-driven Prime Focus LMT

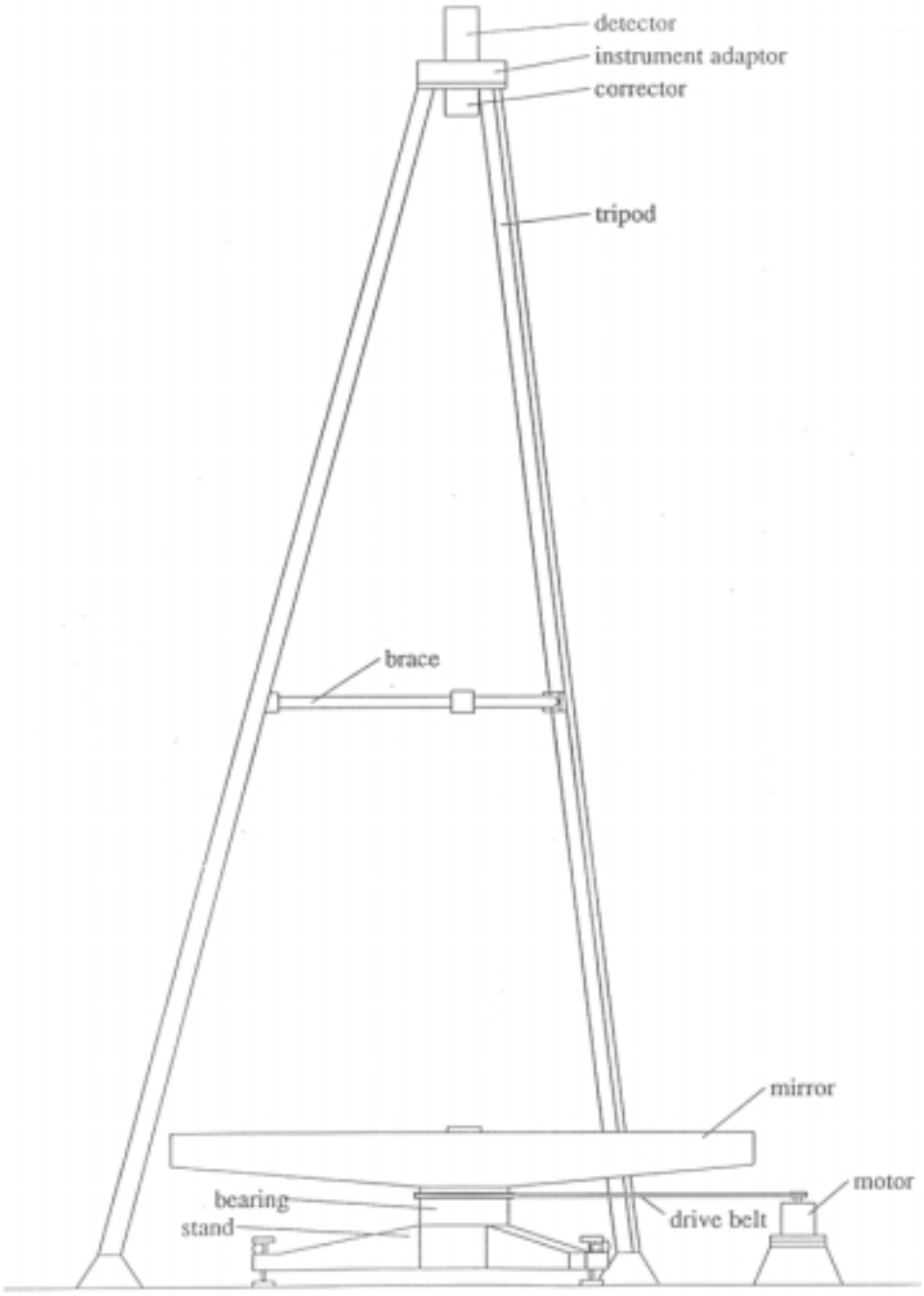

Figure I-4. Schematic drawing of the UBC/Laval 2.7 m diameter belt-driven LMT showing the mirror, bearing and substructure, as well as the prime focus superstructure.

Epsilon Lyrae (2.3 and 2.6 arcsecond pair) in trailed photographic images taken at the prime focus above the mirror. This was the first and last astronomical test of a LMT for another 78 years.

Despite his successes Wood abandoned the LMT because of three significant problems. Fundamental from his perspective was the non-utility of a telescope that cannot move, for by its very nature, the LMT must stare at the zenith. Conventional telescopes can point to various celestial objects and track them, but the rotational axis of the LMT must remain parallel to the gravity vector. As described in Chapters III and V, even small deviations from parallelism (>0.1 arcsecond) induce surface waves and optical defects as the mirror's surface begins to deviate from a paraboloid (Borra et al. 1992; Girard and Borra 1997). In his time, Wood could envision only limited usefulness for a zenith staring instrument, but in the present day this is not a serious disadvantage since a variety of contemporary detectors and survey projects are well suited to either mechanical or electro-optical tracking or simple fixed staring.

The advent of the charge-coupled device (CCD) (Janesick et al. 1989), with its inherent ability to be read line by line, analogous to photographic film on a conveyor, has enabled LMTs to be used for astronomical surveys requiring the imaging of long strips of the sky on a nightly basis (McGraw et al. 1980). Using CCDs, like that shown in Figure I-5, it is possible to track celestial objects electro-optically, rather than mechanically, and thus straightforwardly create moderate duration (30-200 second) time exposures of contiguous transiting star fields at the focus of a fixed telescope without trailing (Figure I-6). The effective exposure time is simply the field crossing time for sidereally drifting

LSP 2K CCD and Data Acquisition Electronics

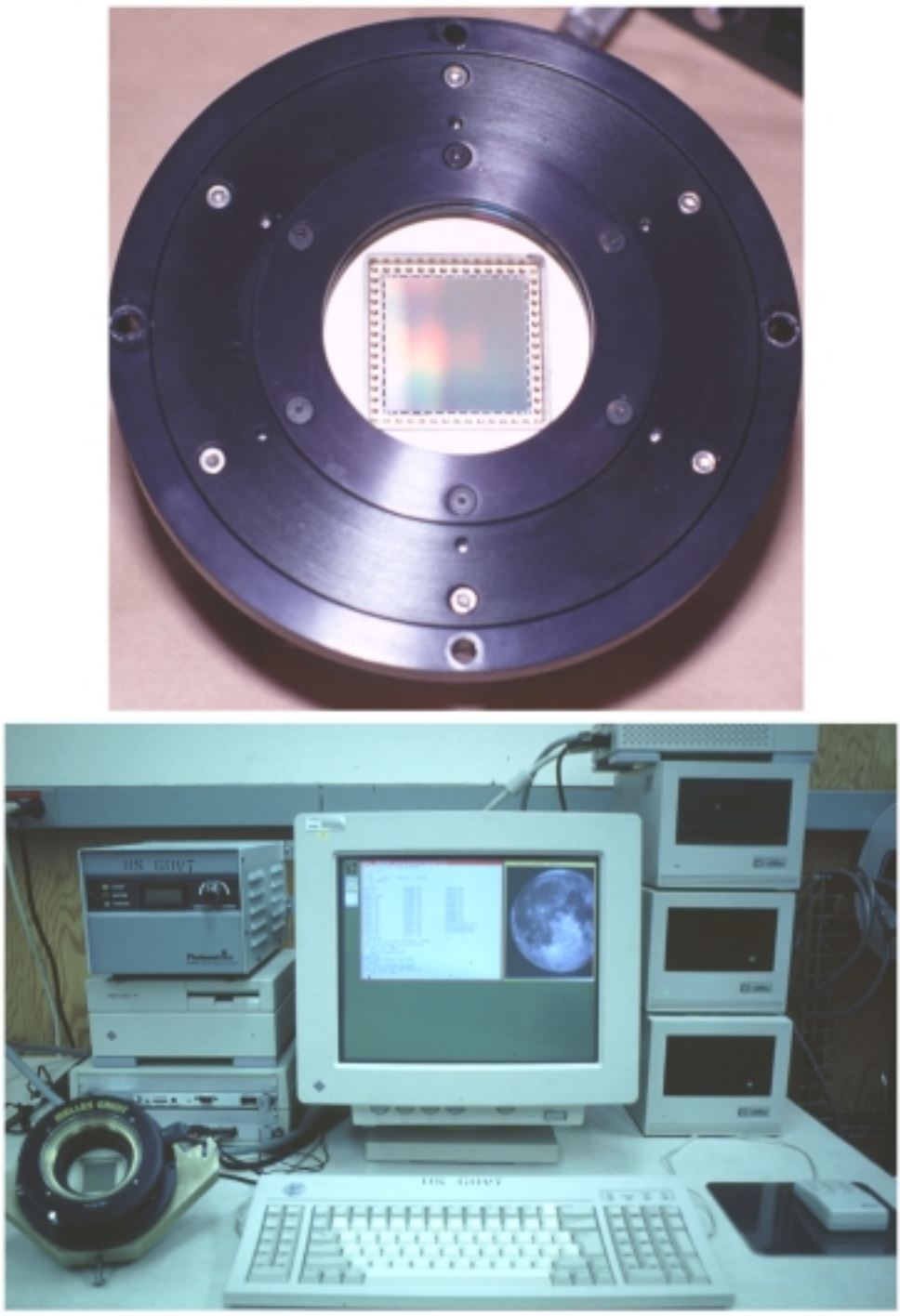

Figure I-5. View of the Lick-Smithsonian-Photometrics (LSP) 2K CCD and support equipment used with the NASA-LMT during the1994 through1997 observing seasons. This 15 micron pixel 2048x2048 array CCD yielded a 20.33 arcminute wide field of view. The computer system has since been upgraded and the LSP 2K CCD has been replaced with 1K and 2K CCDs with higher quantum efficiency.

NASA-LMT: Sidereal Drift-Scan Image with LSP 2K CCD

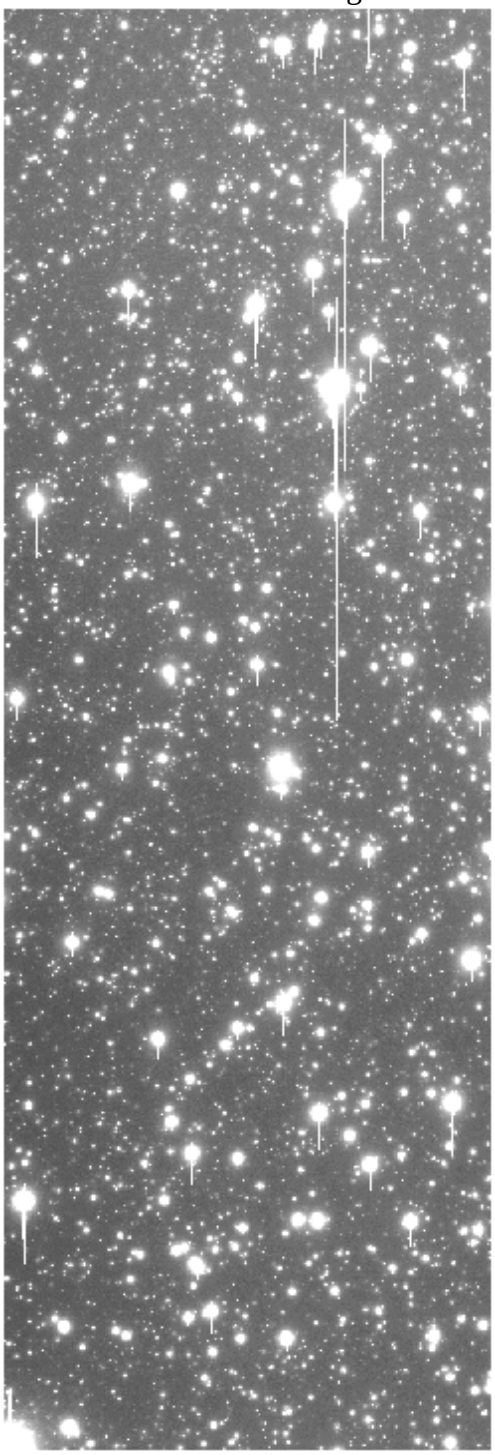

Figure I-6. NASA-LMT sample sidereal drift-scan image of a star field at low galactic latitude acquired with the LSP 2K CCD at NODO. The image measures 20.33 x 61 arcminutes and the effective exposure time is 97.1 seconds giving a white-light limiting magnitude of approximately 22. During routine astronomical observations image strips of >100 degree length are frequently obtained. North is left, West at top.

celestial or other objects (ie. orbital objects) moving through the telescope field of view (FOV). This drift scanning or time delay integration (TDI) technique has applications ranging from Near Earth Object (NEO) searches (Gehrels 1991) to Orbital Object Research (Henize et al. 1994; Mulrooney 1993) to Astronomy (Benedict et al. 1995). It has also been successfully applied to the LMT (Hickson et al 1994; Mulrooney 1995; Hickson and Mulrooney 1998a).

The CCD or other detector can also be mechanically transported across the field of view at the sidereal rate, then reset to the field edge, and the process repeated indefinitely. This generates a discontinuous strip of sky but is effective when acquiring data with Infrared (IR) cameras (which cannot perform TDI) or when using fiber-boules for fiber-fed spectrographs (Weedman et al. 1987). This transport capability is currently being enabled at the NASA-LMT to support proposed IR observations.

In the case of image-intensified video orbital debris survey work (Potter and Mulrooney 1997; Africano et al. 1999) or LIDAR (light detection and range-finding) applications (Sica et al. 1995, Wuerker 1997), where there is no requirement for object tracking, a zenith staring LMT is perfectly suitable. The NASA-LMT's primary mission to survey and characterize the small (1 to10cm diameter) orbital debris population is being fulfilled via the fixed staring mode. Figure I-7 shows an orbiting object transiting the NASA-LMT field of view. In this instance, the detector employed is a commercial digital video camera optically coupled to a 40 mm diameter Micro-Channel Plate (MCP) image intensifier. Other examples are shown in Chapter VI.

The issues of bearing stability and motor-driven rotational velocity stability also

NASA-LMT: Video Images of a Transiting Orbital Object

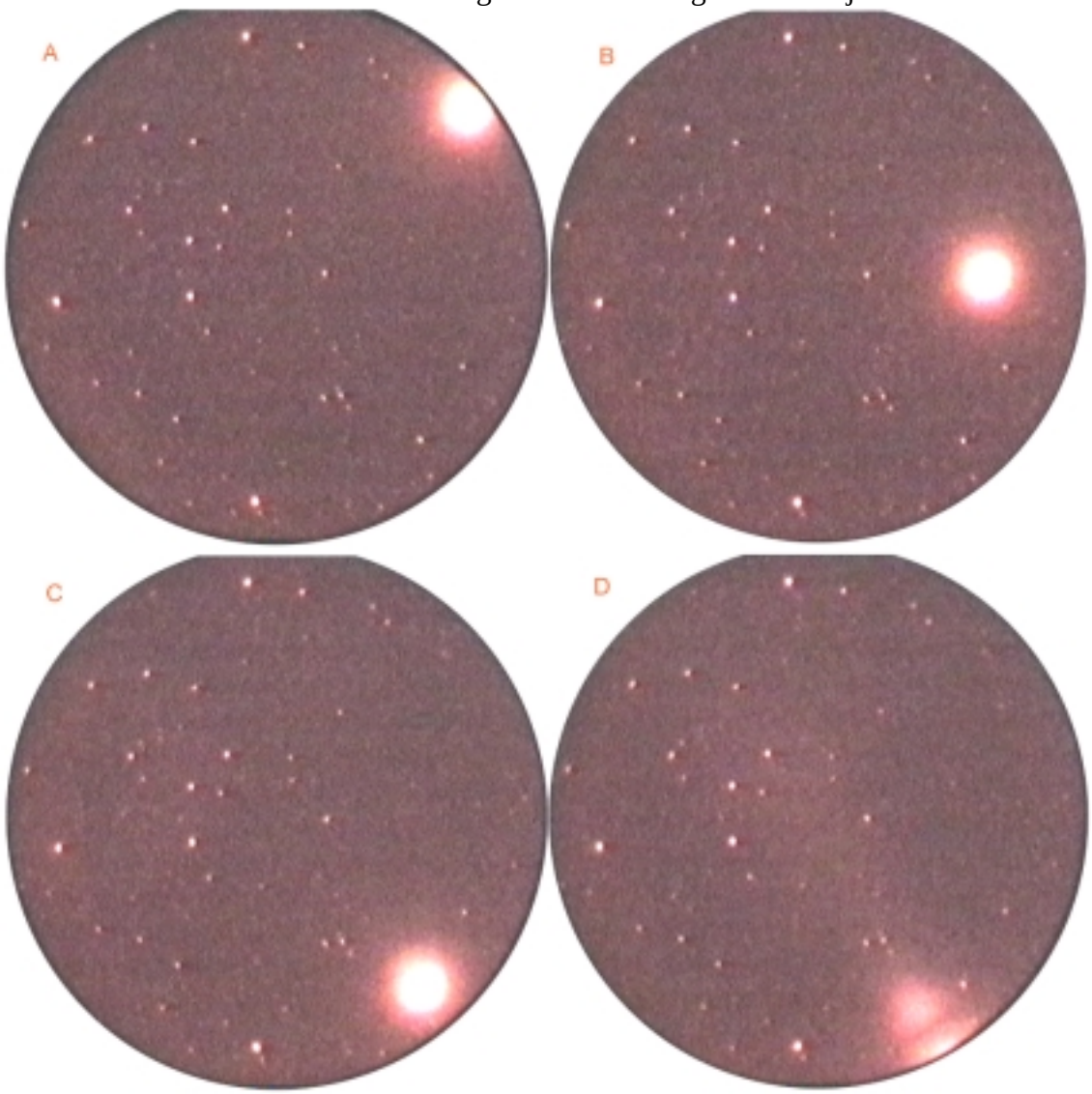

Figure I-7. Time series of video images acquired with the NASA-LMT using a Micro-Channel Plate (MCP) intensified digital video camera. The field of view is 0.444 degrees in diameter. The interval between frames is 0.13 seconds which yields an angular velocity for the object of approximately 1.07 degrees/sec. Assuming the object is in a circular orbit, this corresponds to an altitude of 410 km. By calibrating the image using field stars of known brightness and assuming an albedo and phase function, the object size can be obtained. Alternately, if the object is of known size, the geometric albedo may be obtained for an observation at a single solar phase angle. The limiting apparent magnitude with this detector is 17.

presented a severe challenge for Wood. Under ideal circumstances, the mirror should be capable of diffraction-limited performance. This requires that the liquid mirror surface be parabolic to the Rayleigh eighth-wave criterion which states that the root-mean-square (rms) deviation from a parabolic surface not exceed one eighth of a wavelength of light ($\lambda/8$ where λ = 400 to1000 nm in the optical region). This constraint can be relaxed marginally in practice since atmospheric seeing introduces wave front errors of several waves (Fried 1966; Tatarski 1961). The mirror figure should nonetheless be as accurate as possible to insure that performance is primarily limited only by atmospheric seeing rather than directly preventable optical defects. Mechanical bearings, as employed by Wood, tend to have large coning errors (>>1 arcsecond) which gives rise to mirror wobble and therefore an inaccurate figure. They also generate significant acoustical frequency vibrations that create waves on the mirror surface (Wood 1909; Tremblay and Borra 2000). These attributes make them unsuitable for use in generating astronomical quality liquid mirrors. Air bearing platforms conversely, with their inherently low levels of coning error (~0.02 arcsecond), vibration (<10 nanometer (nm) @10Hz), and internal friction, have completely eliminated bearing induced problems with mirror surface quality (Dahl PC). Additionally, crystal-stabilized synchronous motors have successfully eliminated the velocity drift inherent in the non-synchronous motors of Wood's era and the resultant focal length instability has been rectified. Unfortunately other more recalcitrant sources remain for surface waves and focal length changes as detailed in Chapter III. .

After Wood's research, LMT work paused for more than 70 years until Ermanno

Borra approached the issue with the aforementioned solutions to the three main problems in mind: CCDs, air bearings, and synchronous motors (Borra 1982). From 1982 to the present he has created many experimental LMTs in his laboratory and in the field at Universite Laval, Quebec, Canada, ranging in size from 1 to 3.7 meters in diameter and with focal ratios from f/0.89 to f/4.7.

The first mirror containers were formed from a stiff plywood disk, surrounded by a metal retaining wall, resting atop an air bearing with a crystal-stabilized synchronous motor and a belt-drive or direct-drive mechanism. Rather than use a flat-bottomed container which would require a large quantity of Hg to form the parabolic surface, Borra followed Wood's original suggestion and created a parabolic substrate atop the wooden blank to minimize the required Hg and thereby both the load on the supporting bearing and the Hg layer thickness - facilitating wave damping as discussed in Chapter III. To do this he poured liquid polyester resin (chosen because it has a lower coefficient of thermal expansion (CTE) than epoxy and better wetting ability with Hg) onto the wooden disk while it was rotating at a speed chosen to yield the desired final focal length. If poured carefully, with minimal air entrapment, the epoxy resin cured into a smooth parabolic substrate of the proper focal length upon which the Hg would reside. In this way, the final mirror in rotational equilibrium contains only enough Hg to cover the parabolic substrate with a uniform layer, rather than wastefully filling a flat-bottomed container (Borra et al. 1985).

Borra's later mirrors, including the most recent 3.7m (Tremblay and Borra 2000), utilize the same spun-cast parabolic surface, but with a composite substructure replacing

the plywood. This composite structure, consisting of foam, Kevlar sheets and epoxy, provides a high stiffness-to-weight ratio that is essential for larger mirrors to prevent them from flexing under the weight of the Hg layer. Composite mirror construction was pioneered by Hickson (Hickson et al. 1993) following his experiences with composite aircraft. The NASA-LMT and others discussed later in this chapter, all use composite mirror containers built by Hickson and spun-cast upper surfaces that were formed in-situ. Figure I-8 shows a cross-sectional view of the NASA-LMT mirror container and Figure I-9 illustrates the spin-casting process.

The introduction of the spun-cast polyester surface enabled uniform and thin (< 5mm) Hg surface layers to be used. This not only reduced the weight of the mirror and thus the load on the air bearing, but also dramatically improved the wave damping characteristics of the mirror. As discussed in Chapter III, thin fluid layers damp waves more effectively than thick layers (Girard and Borra 1997; Content 1992; Tremblay 1999). Thin layers could only be used however if a channel was employed at the outer perimeter of the mirror surface. Liquid Hg has high surface tension that causes thinner layers to separate from the mirror's edge. Borra et al. (1992) employed a 5 mm deep, 4 cm wide, channel that acts as a reservoir to which the thin Hg layer can attach. Without it the Hg will not spread over the parabolic substrate and form a smooth stable surface - it will simply form individual puddles. Figure I-10 shows the perimeter channel of the NASA-LMT before and after filling and the pooling behavior of isolated Hg on the mirror's surface.

As shown in Figure I-11, forming the mirror surface was initially accomplished

NASA-LMT: Cross-section of Mirror Container

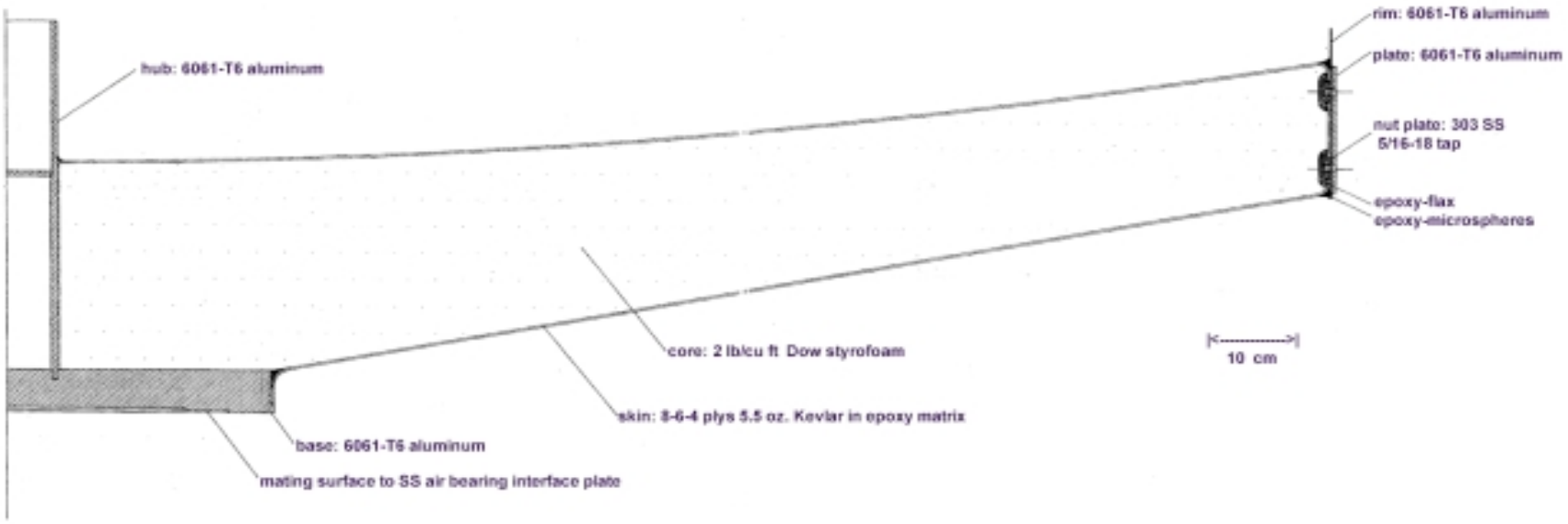

Figure I-8. A cross-sectional view of the 3 meter diameter NASA-LMT mirror container showing the composite structure. The mirror consists of a sectional foam core centered on an aluminum hub. The foam core is covered top and bottom with epoxy and microsphere impregnated Kevlar sheets. A 5mm thick parabolic coating of polyurethane is generated on the upper surface via spin-casting. The container is lightweight (160 kg) and sufficiently stiff to support a 5mm thick Hg layer (460 kg). It was designed and built by Paul Hickson at the University of British Columbia (UBC).

NASA-LMT: Spin-casting the 3.0 m Mirror

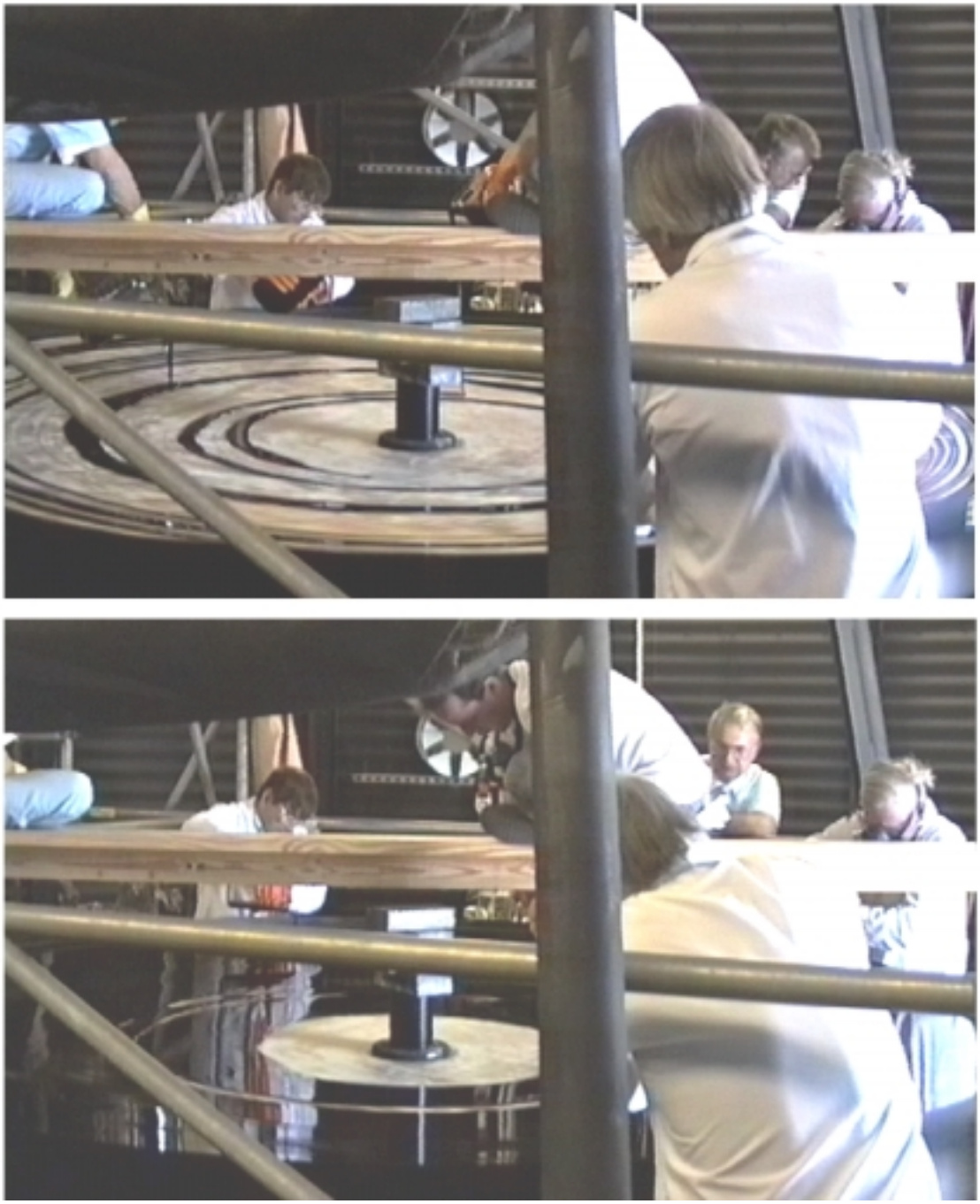

Figure I-9. Time series illustrating the spincasting process at NASA-JSC. Liquid polyurethane is poured onto the mirror container while it is rotating at the appropriate angular velocity (1.043107 rad/sec) for the design focal length (4.511 m). The polyurethane is poured by six individuals into each of six equal area annuli to insure an even distribution. A plank is used to access the mirror center. The polyurethane fully cures to yield a parabolic surface within 4 hours. As discussed later, in Chapter VI, there is some evidence of print-through to the final Hg surface of the boundary between the six annuli.

NASA-LMT: Perimeter Channel

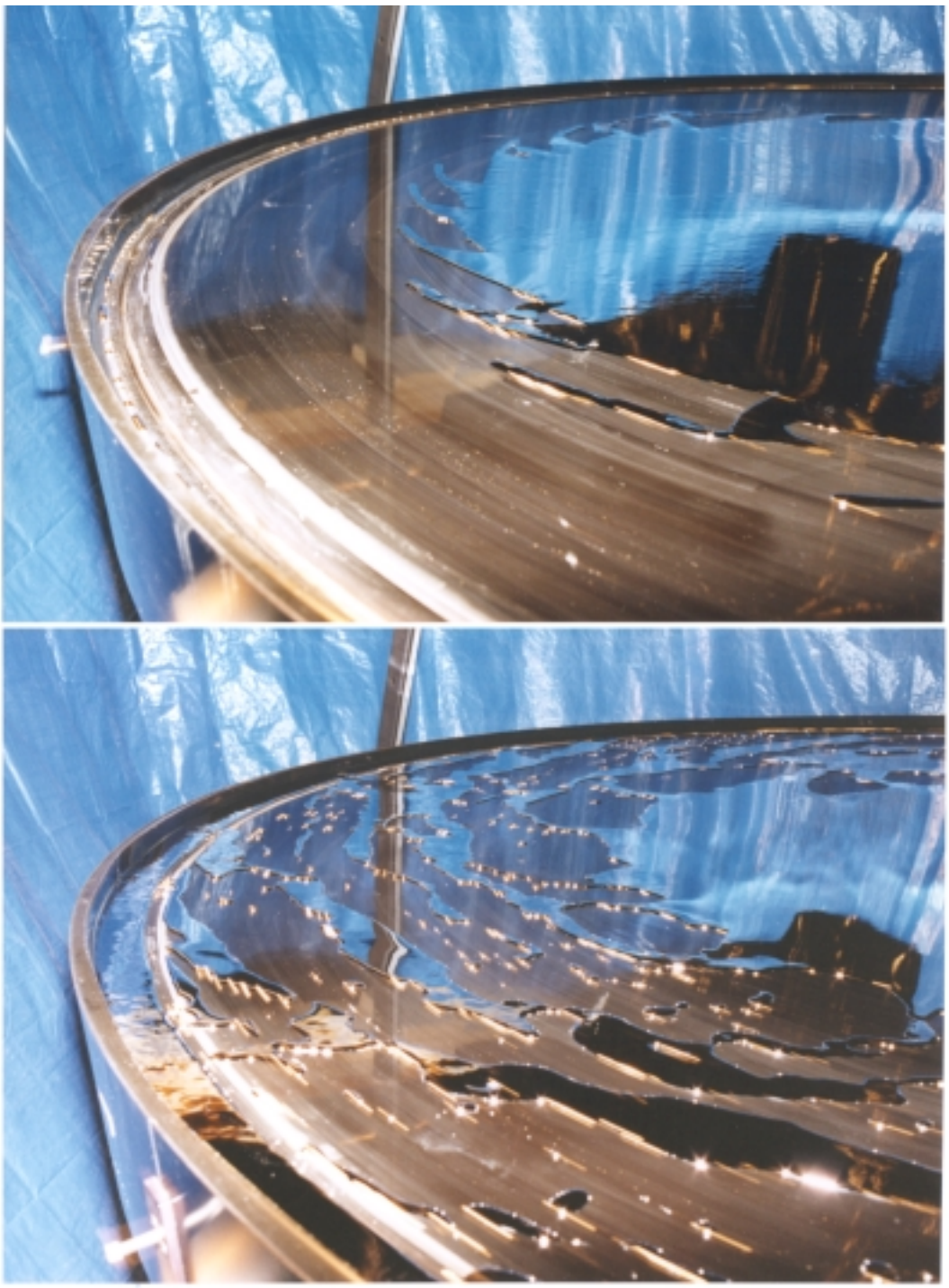

Figure I-10. The perimeter channel of the 3 meter NASA-LMT before and after filling with Hg. The channel provides a 2.8 liter reservoir to which the thin (<5 mm) Hg film covering the mirror surface can attach without breaking away from the mirror rim. The channel is approximately 4 cm wide and extends 0.75 cm below the parabolic surface. A similar channel surrounds the mirror central hub and performs the same function.

Laval Universite 1.5 meter Liquid Mirror: Hg Surface formation

Figure I-11. Hg surface generation with the Universite Laval 1.5 meter diameter Liquid Mirror. Mylar sheets hung from rods of various length are used to manually spread the Hg gradually inward from the mirror's outer edge. The mirror is slowed from an over-speed condition to facilitate the process. The technique is time consuming and frequently must be restarted when a tear develops before completion. Luc Girard's angular momentum method is significantly more efficient and has supplanted this technique.

using a laborious technique in which Mylar sheets were used to coax and spread the Hg over the container surface. Starting from an over-speed condition in which the Hg was collected into an annulus at the perimeter of the mirror container, the mirror was gradually slowed to its design speed while two Mylar sheets were used to manually spread the Hg layer inward toward the container's center. This process was time consuming and had to be restarted from the beginning if a tear occurred in the spreading Hg layer (Borra et al.1992).

Borra's graduate student Luc Girrard devised a much more efficient method for establishing Hg layers as thin as 1.4 mm. In this method, the mirror is rotated manually by a person holding the edge of the mirror container. Variable angular rates are used to spread the Hg over the surface in an interactive process which, once mastered, takes only a few minutes to complete. This technique is used at the NASA-LMT to routinely establish Hg layers as thin as 1.4 mm and is described more fully in Chapter V. Even thinner layers (<1mm) require Hg to be slowly pumped from the mirror surface after it has been formed, via a small tube inserted at the mirror's center (Borra et al. 1992). Girard and Borra (1997) have achieved a 0.5 mm Hg layer thickness in this way.

Before using Hg exclusively, as employed in the earlier LMTs, Borra experimented with various reflective fluids for the mirror surface, including mercury, gallium (Ga), and gallium alloys. Hg, despite its toxicity, was chosen because its oxide is transparent. Both Hg and Ga readily oxidize in air, but Ga forms a translucent oxide coating of poor reflectivity. Hg, however, forms a transparent oxide coating that also inhibits evaporation (Byers and Gibbons PC, Hickson PC, Borra et al. 1992). As

discussed in more detail in Chapter IV, Hg has excellent reflectivity of approximately 75% in the optical region and 90% in the near infrared (Borra 1982) and it remains a liquid above -38 degree Centigrade - essential for LMTs operating in the cold environs typical of high-altitude observatories.

Through extensive knife-edge, Hartmann, and interferometric measurements, Borra et al. (1992) have exhaustively characterized mirror quality as a function of Hg layer thickness, mirror-axis tilt, and various diaphragm masks. Mean Strehl ratios of ~ 0.6 androot-mean-square (rms) wave front deviations from a perfect parabola of $\sim\lambda/20$ at 632.8nm have been obtained by using extremely thin Hg layers (<1.5mm), accurate alignment of the rotational axis with gravity (<0.25 arcsecond), and by masking the outer edge of the mirrors (Girard and Borra 1997; Figure I-12). Masking partially obscures wave activity which is more pronounced in the thicker Hg layer at the mirror's edge than over the surface in general. The edge layer is thicker because of the perimeter channel and the slight mirror deformation from the weight of the Hg (the mirror is spun-cast with no Hg fluid load). Borra and Girard (1997) have shown that the mirror edge is the dominant source of scattered light in test source point-spread-functions (PSFs). Wave activity as observed on the NASA liquid mirror and possible generation mechanisms are described in detail in Chapter III.

In addition to laboratory testing, Borra's group obtained 200 hrs of field astronomical observations with a 1.2 meter f/4.58 LMT setup near Quebec City, Quebec. This instrument produced respectable ~2 arcsecond full-width-half-maximum (FWHM) resolution trailed star images on 35 millimeter (mm) photographic film. The data

Scatterplate Interferogram and 3D Surface Rendering of a Liquid Mirror

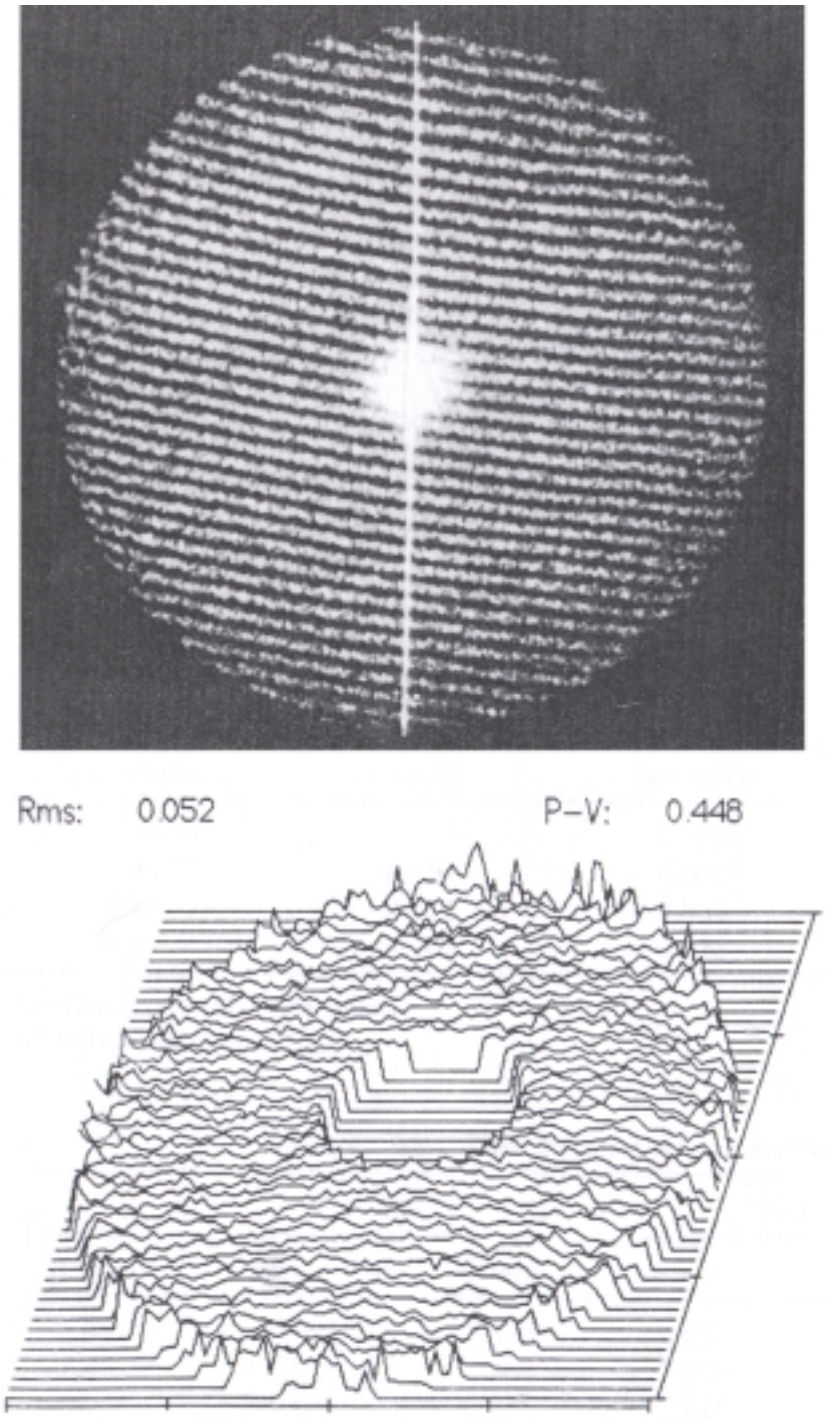

Figure I-12. Interferometric testing of a laboratory Liquid Mirror (LM). The upper image shows the typical interference pattern of a LM acquired with a scatterplate interferometer. The lower figure is the resulting instantaneous three dimensional surface rendering generated of a 2.5 m f/1.2 LM with a 0.85 mm Hg layer. It indicates an RMS wavefront error of approximately 1/20th of a wave of 632.8 nm light (Helium-Neon Laser). (Girard and Borra 1997)

obtained was analyzed for optical flares and flashes - generating the first astronomical paper based on data obtained solely from a LMT (Borra et al. 1988). This field telescope was one of the precursors to a collaborative effort between Hickson's group at the University of British Columbia (UBC) and Borra's group at Universite Laval: the UBC/Laval 2.7m f/1.89 LMT (Hickson et al. 1992). This instrument operated for several seasons from 1994 to 1997 from two sites near Vancouver, British Columbia and was the first LMT built as a test-bed for intensive astronomical research.

The UBC/Laval telescope consisted of a 2.7m diameter composite mirror (Figure I-13) with a spun-cast polyester parabolic substrate resting atop an air bearing coupled to a synchronous motor via a Mylar drive belt. It contained approximately 11.5 liters of liquid Hg yielding a 2 mm surface layer - thin enough to provide moderate wave damping characteristics. A 2048x2048 15 micron (um) pixel CCD camera was located behind a 5-element field corrector at the prime focus position. The corrector lens was employed to remove coma and astigmatism from the fast f/1.89 parabolic primary. The telescope was initially housed in a silo structure near sea level and then later moved to a hilltop site in the UBC research forest (~450 m AMSL). Hickson designed and built the observatory at the new site for the 6 meter LZT (Hickson et al. 1998). The 2.7m UBC/Laval telescope was housed there only temporarily in 1996 to finalize a survey project involving BVRI imagery.

During most of its working life this telescope acquired sample data to demonstrate the feasibility of a narrow-band spectrophotometric survey conceived by Hickson (Hickson et al 1994). The LMT observed a 20 arcminute wide strip of sky centered at a

UBC/Laval 2.7 m LMT: Overhead View

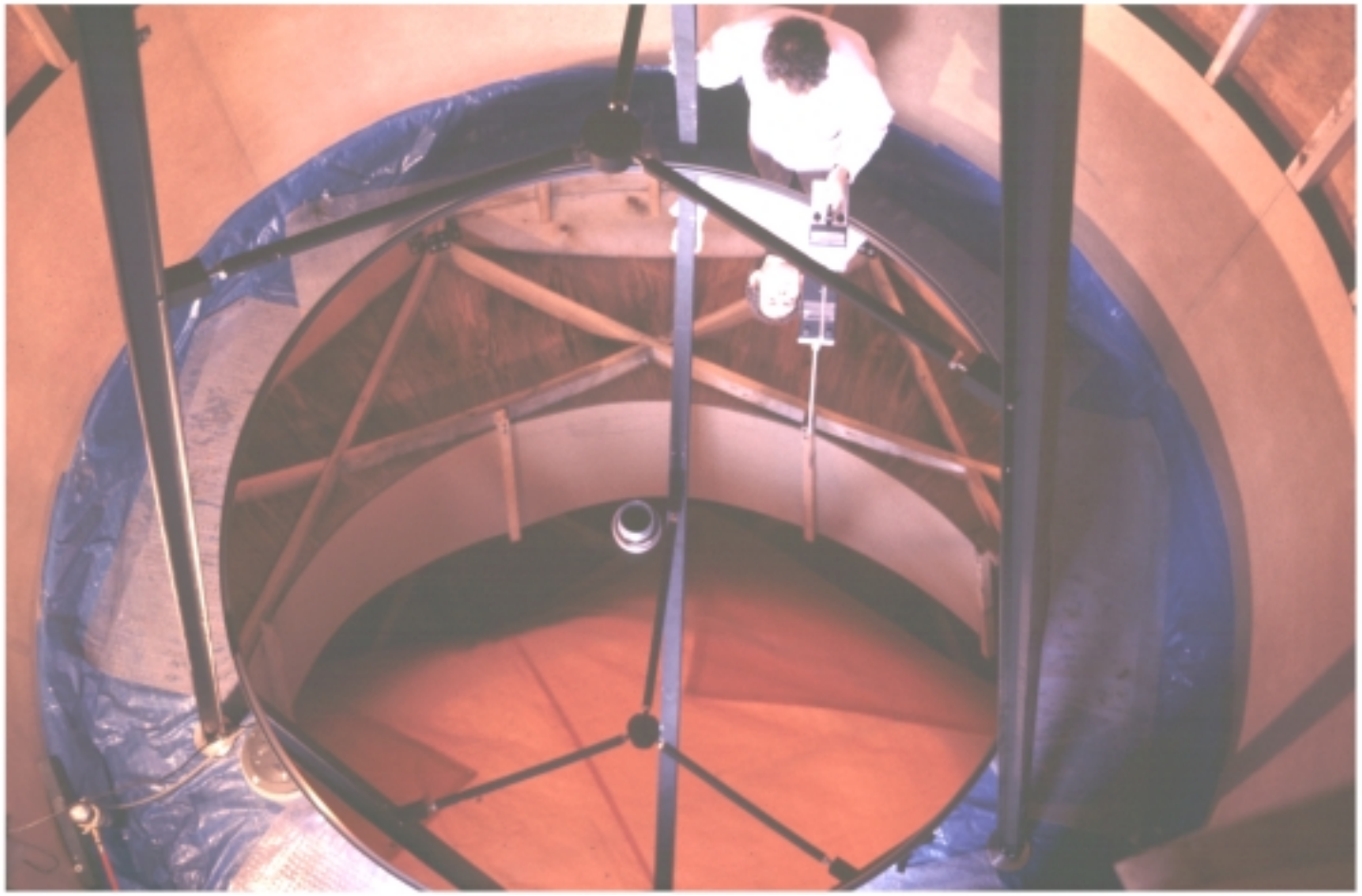

Figure I-13. An overhead view of the UBC/Laval 2.7 meter diameter LMT – the first LMT to conduct routine astronomical observations. Paul Hickson holds an instrument used to measure the Hg vapor concentration. The mirror is fully oxidized and Hg emissions are zero, hence the absence of respiratory protection. Photo courtesy Paul Hickson.

49 degree Declination (Dec) spanning 6 hours of Right Ascension (RA) at high galactic latitude. The 5.0 meter focal length yielded a 0.6 arcseconds/pixel plate scale and a 129 second effective exposure time for the 2048 row CCD operating at the 49 degree Declination band. The telescope routinely achieved resolution of 1.5 to 2.0 arcsecond FWHM. The main objective was to obtain spectral energy distributions (SEDs) for all galaxies and quasars within the survey strip. Using high resolution SEDs obtained by imaging the survey strip each night through one of 40 different optical narrow-band interference filters, the redshift and morphology of each object with a limiting R magnitude of 21 could be determined. Inclement weather and generally poor seeing hindered the results. With advent of the NASA-LMT in 1995, efforts shifted to performing the survey with this new larger LMT located at NODO - a good astronomical site (Hickson and Mulrooney 1998a). Those efforts have been successful and are described in Chapter VI.

Immediately following the early success of the UBC/Laval LMT in 1994, the University of Western Ontario (UWO) developed a 2.65 meter LMT-LIDAR (Laser Detection and Range-finding) using a mirror designed and built by Hickson (Sica et al. 1995). The LMT is used with a gated photomultiplier as the collector for the return light emitted by florescing atomic and ion species in the upper atmosphere. These species are excited by a high-power ground-based laser located adjacent to the LMT. An antenna field is also co-located to induce electromagnetic effects on the ionosphere. The LIDAR studies the concentration, motion, and altitude distribution of these species by timing the emitted and received light pulses and measuring their intensity. The method is analogous

to RADAR operation, hence the acronym LIDAR. The UWO-LIDAR has operated successfully for 6 years - making it the oldest continually operating non-astronomical LMT.

A second LMT-LIDAR was built in 1995 by the University of California Los Angeles (UCLA). The UCLA-LIDAR is located near Fairbanks, Alaska, under the auroral oval, and uses a 2.7 m f/1.67 mirror container built by Hickson (Wuerker 1997). It incorporates a Mylar belt-drive and an air bearing identical to that used with the NASA-LMT. This LMT operates in a closed observatory environment - observations are made through a high-quality float glass window that covers the observatory. The instrument hasoperated routinely and successfully since 1995 and is illustrated in Figures I-14 and I-15.

Success with the UBC/Laval and NASA-LMTs lead Hickson in 1993 to conceive of a larger aperture instrument. The 6 m f/1.5 LZT is scheduled to begin preliminary observations in the Spring of 2001 (Hickson et al. 1998). Its primary mission is the continuation of the spectrophotometric survey work performed with the UBC/Laval and the NASA-LMT. Using a 2048x2048 CCD giving 103 second effective exposures, it will obtain SEDs to a limiting R magnitude 25.4 over a 24 arcminute wide field of view.

The LZT differs from previously built LMTs in several respects. As shown in Figures I-16 and 17, it incorporates a light-weight space frame mirror design with a tubular steel substructure and bonded hexagonal mirror segments forming the mirror surface. Adjustable support points will enable the mirror surface to be maintained parabolic to within 0.1 mm, better than what can be obtained by spin-casting and

UCLA 2.7 m Liquid Mirror LIDAR

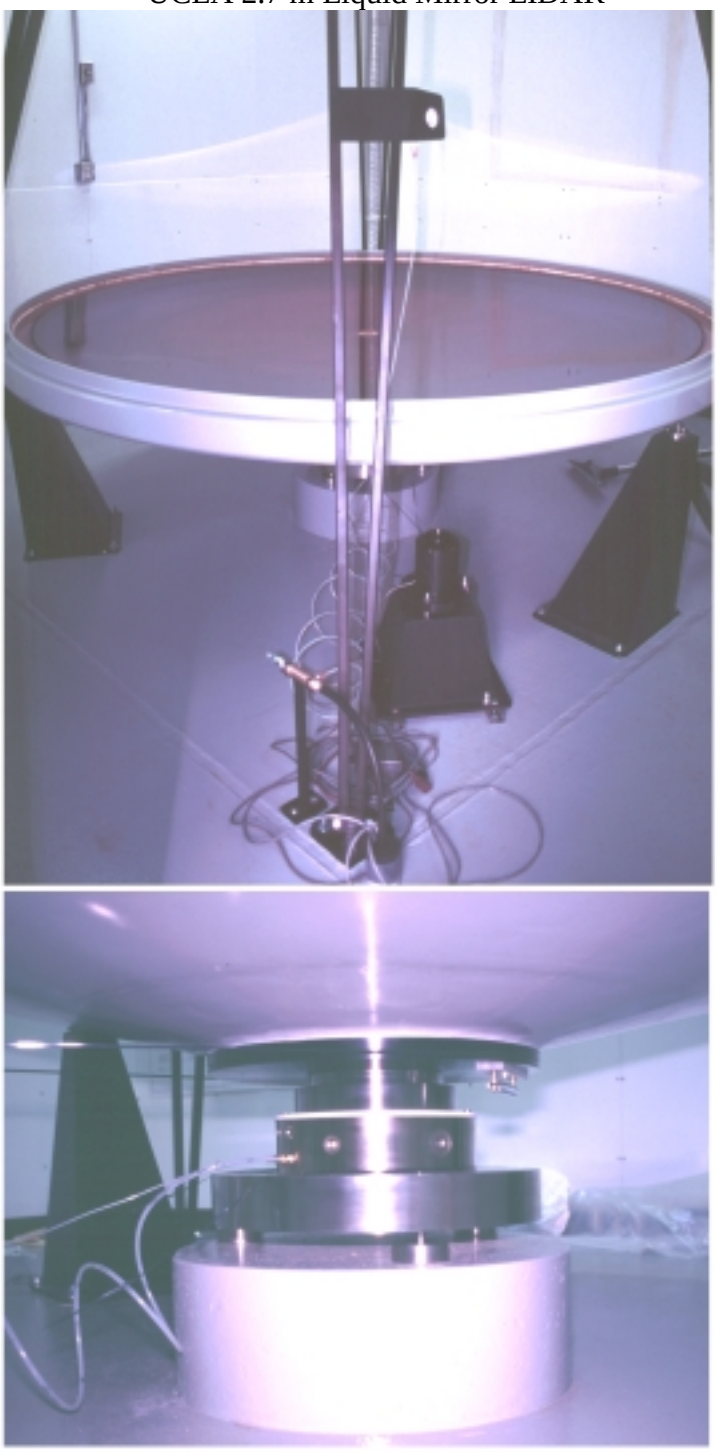

Figure I-14. Upper and lower views of the UCLA 2.7m Liquid Mirror LIDAR located in Fairbanks, Alaska. The polyethylene mirror surface is visible as Hg has not yet been introduced to the mirror container. The belt and belt-drive motor are visible at left of center in the upper photograph. The towers (black) insure against catastrophic mirror tilt. The air bearing itself is identical to that used with the NASA-LMT.

UCLA 2.7 m Liquid Mirror LIDAR

Figure I-15. The UCLA 2.7m Liquid Mirror LIDAR located in Fairbanks, Alaska. The upper photograph shows the spinning mirror with its parabolic Hg surface. The lower image shows the compact observatory whose roof consists of a transparent float glass window through which the Liquid Mirror observes. The principal investigator, Ralph Wuerker, is at far left.

6.0 m UBC-Large Zenith Telescope (LZT): Mirror space-frame assembly

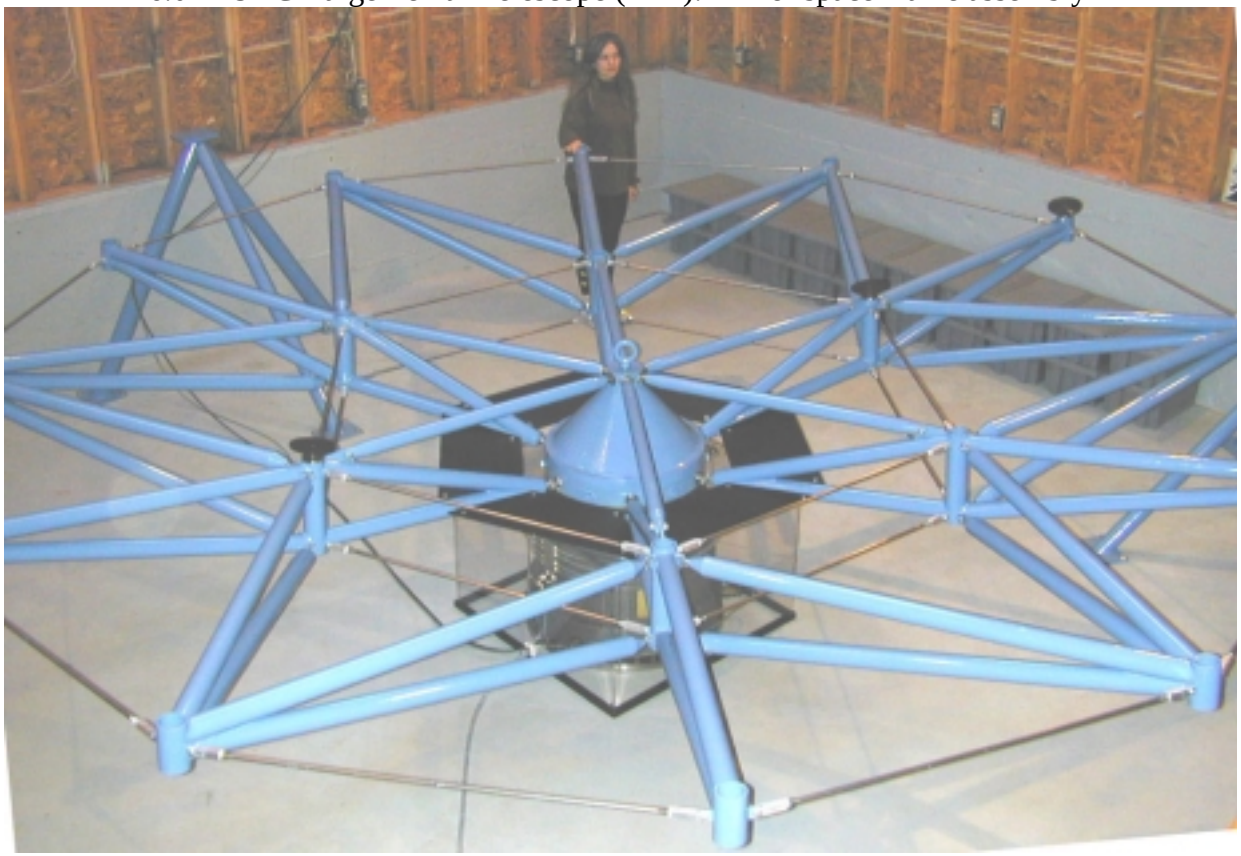

Figure I-16. The 6.0 meter diameter Large Zenith Telescope (LZT) designed and built by Paul Hickson at the University of British Columbia (UBC). The space frame design of the mirror substructure is an alternative to the monolithic composite construction presently employed in LMT primary mirrors. A thin composite membrane will be placed atop the space-frame and will be supported by floatation pads that can be adjusted to give an overall parabolic figure to within a +-0.1 mm surface deviation. The final mirror will support a 1mm (or thinner) Hg layer and operate at f/2. The Professional Instruments Company (PICo) air bearing, which was specially designed for this project, is enclosed in a plexiglass cover beneath the structure. It can support a 9,000 kg axial load - sufficient for an 8 meter LMT. Photo courtesy Paul Hickson.

6.0 m UBC-Large Zenith Telescope (LZT): Mirror space-frame assembly

Figure I-17. Assembling the space frame for the 6.0 meter diameter Large Zenith Telescope (LZT). Several floatation pads which will support the mirror membrane are visible. The PICo 20R air bearing is seen with the plexiglass protective cover not yet installed. Photo courtesy Paul Hickson.

enabling extremely thin Hg layers (~0.5mm) to be formed. The air bearing is now installed and is a much larger version of that employed on the NASA-LMT. It is capable of supporting an 8 m diameter liquid mirror. Interestingly, the 4-element corrector design contains two de-centered wedged elements for removing star trail curvature caused by the small circle stellar motion (Hickson and Richardson 1998). The trail curvature causes stellar images to spread orthogonally to the CCD read direction during drift scanning since the stars move along curved trajectories rather than straight lines at non-equatorial latitudes. This is discussed in more detail in Chapter IV.

The most recent LMT project is lead by Jean Surdej who has assembled a group of Belgian astronomers and engineers, along with Ermanno Borra as a key advisor, to build a 4 meter LMT for use in Chile. This LMT will be used for astronomical surveys and benefits from the extensive laboratory and observational experience preceding it.